

# Ultrastructural Study of Tooth Enamel with Amelogenesis Imperfecta in AI-Nephrocalcinosis Syndrome

P. PHAKEY,<sup>†‡</sup> J. PALAMARA,<sup>†‡</sup> R. K. HALL,<sup>§</sup> and D. A. MCCREDIE<sup>||</sup>

<sup>†</sup>Department of Physics, Monash University, Melbourne, Australia; <sup>‡</sup>School of Dental Science, University of Melbourne, Australia;

<sup>§</sup>Department of Dentistry, Royal Children's Hospital, Melbourne, Australia; <sup>||</sup>Renal Unit, Royal Children's and Royal Melbourne Hospitals, Melbourne, Australia

(Received August 8, 1994; accepted August 29, 1994)

This paper describes the ultrastructure of the affected enamel and the clinical features in two siblings with the syndrome of nephrocalcinosis and amelogenesis imperfecta. Nephrocalcinosis was diagnosed by intravenous pyelography, and confirmed by ultrasonography and CT scan. Amelogenesis imperfecta AI was diagnosed clinically and histologically.

Light microscopy showed that the affected enamel surfaces were rough and the enamel was hypoplastic and mainly positively birefringent. Scanning electron microscopy revealed a rough and extensively cracked enamel surface covered with oval shaped blister-like protrusions. TEM showed porous enamel consisting of loosely packed and randomly oriented thin ribbon-like crystals with little or no prismatic structure.

Observations showed that hypoplasia together with hypocalcification and/or hypomaturation defects were present in the same tooth, indicating the possibility of an abnormality in interstitial matrix, leading to dystrophic calcification in the kidney and abnormal tooth enamel formation, or alternatively an involvement of two separate but closely linked genes.

**Key Words:** amelogenesis imperfecta, nephrocalcinosis, hypoplastic enamel, tooth surface, crystal ultrastructure

## INTRODUCTION

Amelogenesis imperfecta (AI) has been classified by Witkop<sup>1</sup> and Witkop and Sauk<sup>2</sup> on the basis of hereditary and pathologic type and by Sundell and Koch<sup>3</sup> on clinical and pathologic appearance. AI usually occurs with a frequency of 1:700<sup>4</sup> to 1:14000<sup>5</sup> persons as an isolated defect with autosomal dominant and recessive as well as X-linked inheritance have also been documented.<sup>6</sup>

Three main pathologic types of AI are: hypoplastic, hypocalcified and hypomaturation. In AI Hypoplasia-type the enamel thickness is reduced. The enamel is either thin, smooth and pitted or is rough, pitted and cratered. AI Hypocalcified-type is considered to be initiated by abnormal primary deposition of crystals causing macroporosities and in some cases a discoloration of the enamel. In AI Hypomaturation-type, it is suggested that disturbances of normal maturation process results in retention of organic protein material within the enamel; thus causing smaller enamel crystallites and abnormal prism structure.<sup>7,8</sup> In many cases however, it is difficult to distinguish between various types of AI.

Nephrocalcinosis is the precipitation of calcium salts in renal tissue and is most commonly found in conditions associated with hypercalcemia and/or hypercalciuria such as renal tubular acidosis, Bartter's syndrome, medullary sponge kidney and in hyperoxaluria. It is being reported with increased frequency as a result of drug induced hypercalciuria, whether from diuretics, steroid therapy or vitamin D.

AI is known to occur as an integral part of several syndromes. Lubinsky *et al.*<sup>9</sup> described a syndrome of AI, nephrocalcinosis, impaired renal concentration and possible abnormality of calcium metabolism citing a paper by MacGibbon<sup>10</sup> which reported affected siblings. A previous investigation by Lubinsky *et al.*<sup>9</sup> demonstrated intrapulpal calcifications in one of his two siblings.

There are very few ultrastructural studies<sup>6,11,12</sup> of AI due to the difficulties associated with preparing ultrathin samples suitable for transmission electron microscopy. The technique of selected-area argon-ion-beam-thinning (AIBT)<sup>13</sup> has proved successful in preparation of ultrathin samples of hard tissue, such that it has been possible to investigate the ultrastructure of healthy enamel,<sup>14-17</sup> early enamel caries<sup>18-20</sup> and the enamel of a particular type of AI which caused pigmented enamel in Polynesian teeth.<sup>21</sup> This investigation describes the ultrastructure of enamel in two siblings with the syndrome of nephrocalcinosis

Address for correspondence: Dr. Roger K. Hall, Dept. Dentistry, Royal Children's Hospital, Flemington Road, Parkville, Victoria 3052, Australia. Tel.: +61.3.813-3350; Fax: +61.3.345-6668

and amelogenesis imperfecta using ultrathin samples prepared by the AIBT technique.<sup>13</sup>

## MATERIALS AND METHOD

One of the permanent incisors (tooth 12 for one of the cases reported here) which had only the incisal edge erupted through the mucosa was kept in a solution of thymol and water and refrigerated. The tooth was then washed in distilled water and air dried for histologic study and ultrastructural investigations using light microscopy, scanning electron microscopy and transmission electron microscopy.

The surface topography of the erupted and unerupted enamel of the tooth was investigated using the whole tooth (prior to sectioning) with a reflected light microscope and with a Hitachi (S/570) scanning electron microscope operating in the secondary electron mode.

For birefringence studies, longitudinal sections were cut with a diamond saw. The cut sections were then hand lapped and polished to an enamel thickness of approximately 80  $\mu\text{m}$ . An Olympus BH polarizing light microscope equipped with a camera attachment, Berek compensator and gypsum first order red plate was used to record the birefringent changes in the specimens in air and after imbibition for several hours in aqueous media. Enamel thickness was measured from the longitudinal sections with the light microscope using a graduated graticule.

Ultrathin sections for transmission electron microscopy were prepared using the improved selected area AIBT technique. It is known that, unlike ultramicrotome sectioning, this method of preparing ultrathin sections results in minimal artifactual change, such as chatter, crystal fragmentation and crystal displacement. A selected area of the sample was enclosed by cementing a slotted grid onto the hand lapped and polished thin section of the tooth. The mounted specimen was thinned in an AIBT unit, to produce an ultrathin sample with a perforation in the area to be examined. The ultrathin samples were examined in a transmission electron microscope (JEOL 200CX) operating at 200KV. Selected area electron diffraction (SAD) patterns were recorded and used in the identification of crystal structure and assessing the crystal orientation.

## OBSERVATIONS

### Clinical Examination

Two siblings were studied with the syndrome of amelogenesis imperfecta (AI) and nephrocalcinosis. The first, a

girl aged 10 years with AI was found to have nephrocalcinosis following investigation of a urinary tract infection. Her asymptomatic brother aged 14 years, also with AI, was then investigated and found to have a similar degree of nephrocalcinosis. Renal biopsies in these two children showed a mild degree of glomerular sclerosis, but the major feature was interstitial infiltration with lymphocytes and plasma cells. Extensive investigations disclosed no metabolic abnormalities and in particular normal levels of serum vitamin D, PTH and osteocalcin. Full details have been reported elsewhere.<sup>24</sup> On the basis of their teeth which were discolored yellow/brown with almost no enamel present (Fig. 1) AI was thought to be Witkop Type IG AI autosomal recessive enamel agenesis type. Nephrocalcinosis was diagnosed by X-ray of the abdomen and intravenous pyelography and confirmed by ultrasonography and CT scan. Extensive investigation of calcium metabolism revealed no abnormality in either sibling. Subsequent development has been normal with no deterioration in renal function. Dentally fibrous gingival overgrowth was marked in both siblings but the female only had an anterior open bite.

### Light Microscopy

The cut section of the teeth showed that the enamel was very thin and in some areas nearly nonexistent (Fig. 2). Although clinically the enamel surfaces appeared smooth, examination of sections with the light microscope (LM) showed that the surface of the unerupted enamel was very irregular (Fig. 3). Measurements using a graticule and from light micrographs showed that the maximum thickness of the unerupted enamel was approximately 0.2 mm which is much less than normal healthy enamel thickness. Examination of polished thin sections, imbibed in air and water, using cross polarizers showed that unlike the normal healthy enamel which is negatively birefringent the affected enamel examined here was positively birefringent (Fig. 3b). Hence the enamel in these teeth was defective and probably porous. However, in some sections, pockets of enamel with negative birefringence were present close to the dentine-enamel-junction (DEJ) (Fig. 3b).

### Scanning Electron Microscopy

Scanning electron microscopy revealed that both erupted and unerupted enamel tooth surfaces were covered with extensive cracks (Figs. 4–6). On the unerupted enamel surfaces ovoid or globular-like protrusions (Fig. 5), similar to tubercles seen on many shells, were present and the cracks were found to be occluded by a thread-like

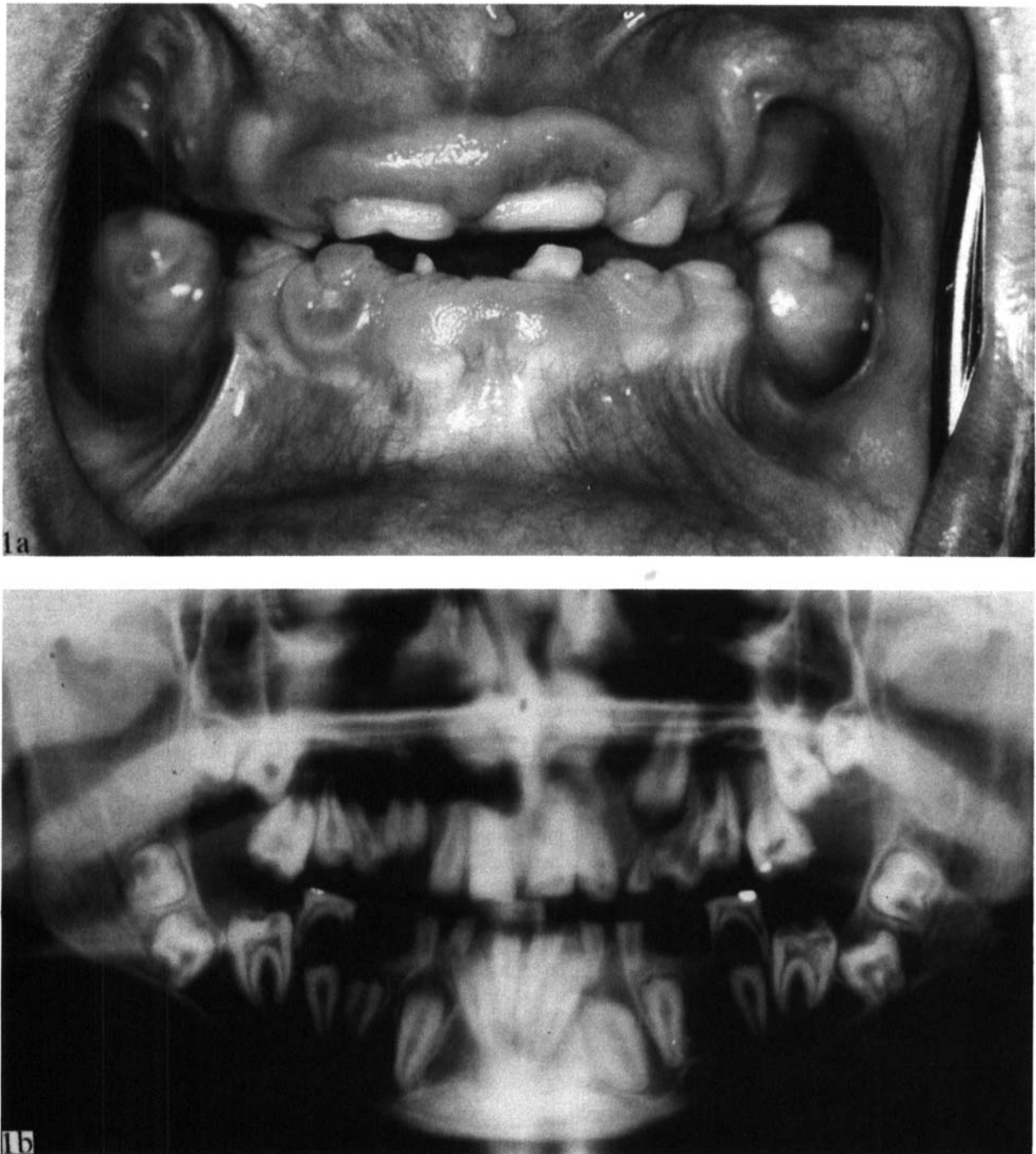


**FIGURE 1** (a) Clinical view of the dentition of a male aged 14 yrs (with almost identical oral abnormalities to those of his sister) showing the worn malformed primary teeth, worn crowns of the permanent incisors and gingival overgrowth (due to pathological follicular remnants). (b) Panoramic radiograph of a male aged 14 yrs showing multiple unerupted permanent teeth with reduced enamel thickness and density and disordered enamel formation also with intracoronal pulp calcification in the lower first permanent molars. Impaction of teeth is also seen.



FIGURE 2 Low magnification transmitted light micrograph of a partially erupted tooth after imbibition in water showing that the enamel (between arrows is much thinner than normal healthy enamel.

material bridging the walls of the cracks (Fig. 6). Some areas of the erupted enamel were smooth in appearance; and in these areas the ovoid or globular-like protrusions were absent (Fig. 4), the cracks were wider and devoid of the occluding material found in the unerupted enamel. This was probably due to exposure to the oral environment.

### Transmission Electron Microscopy

Transmission electron microscopy of ultrathin sections, prepared by the AIBT technique, of the affected enamel (Figs. 7, 8) revealed that the ultrastructure of the erupted and unerupted enamel was very different from normal healthy enamel.<sup>14,15</sup> Unlike normal healthy enamel which consists of long lath-like well packed enamel crystals<sup>14-16</sup> (width ~50 nm) the affected enamel consisted of randomly oriented and loosely packed ribbon-like crystals approximately 10 nm in width (Figs. 7, 8). Occasionally in isolated areas closely packed ribbon-like crystals of

smaller width (~5 nm) were present (Fig. 7). The loose packing of the ribbon-like crystals caused the porosity in the affected enamel. Whether the pores were empty or had an organic or amorphous content could not be determined from the SAD patterns which identified the presence of only a hydroxyapatite phase. The diffuse and continuous nature of the diffraction rings in the SAD patterns of the affected enamel confirmed the small crystal size and their random orientation, respectively. Another characteristic feature of the affected enamel was that the prismatic structure, which is a common feature of normal healthy enamel, was usually absent or was poorly developed such that a pseudo-prismatic arrangement was occasionally seen (Fig. 8a). The SAD pattern of the pseudo-prismatic areas produced diffuse and discontinuous ring patterns (Fig. 8b) indicating small crystal size and some preferred orientation of the crystals in these areas.

### DISCUSSION

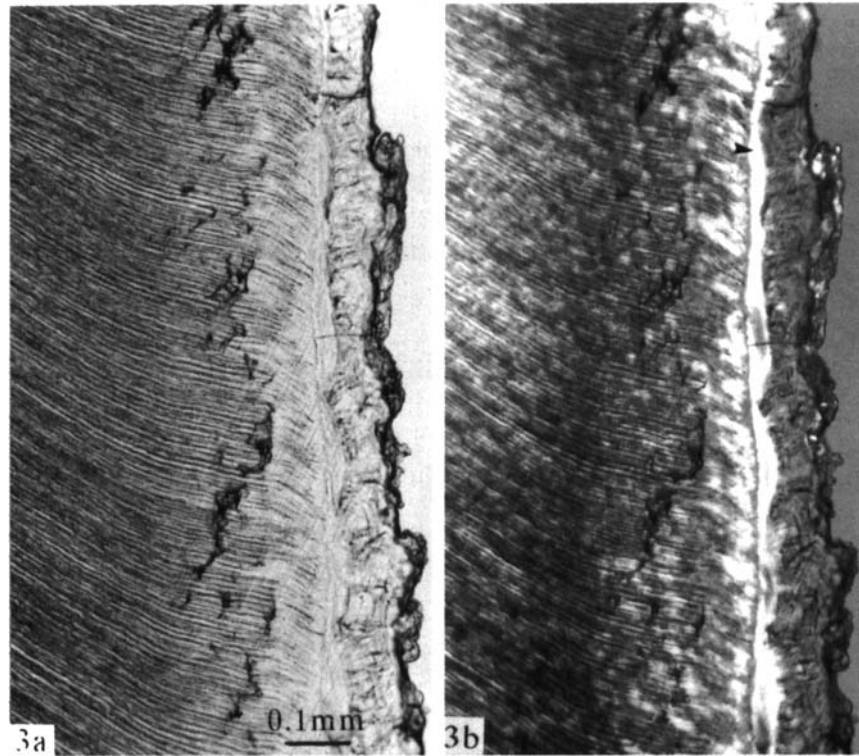
Observations reported here have shown that the tooth investigated had affected enamel which was markedly hypoplastic and defective. The main defects present on the surface of the unerupted enamel of the tooth were ovoid or globular-like protrusions, unevenness of the surface and the extensive cracks with occluding thread-like material. The absence of ovoid or globular-like protrusions on a small area of erupted enamel surface suggested that the affected enamel wore rapidly after exposure to the oral environment; and the enlargement of cracks and the absence of occluding material indicated that the cracks provided pathways into the enamel.

Transmission electron microscopy of affected enamel revealed major ultrastructural differences from the normal healthy enamel, the more common type of hypoplastic enamel,<sup>8,22,23</sup> the polynesian pigmented enamel<sup>21</sup> and other reported AI cases.<sup>6,11,12</sup> The ribbon-like enamel crystals (~10 nm in width) in the affected enamel resembled the immature enamel crystals of normal healthy enamel but were considerably thinner than the lath-like crystals of mature enamel (width ~50 nm). Features like

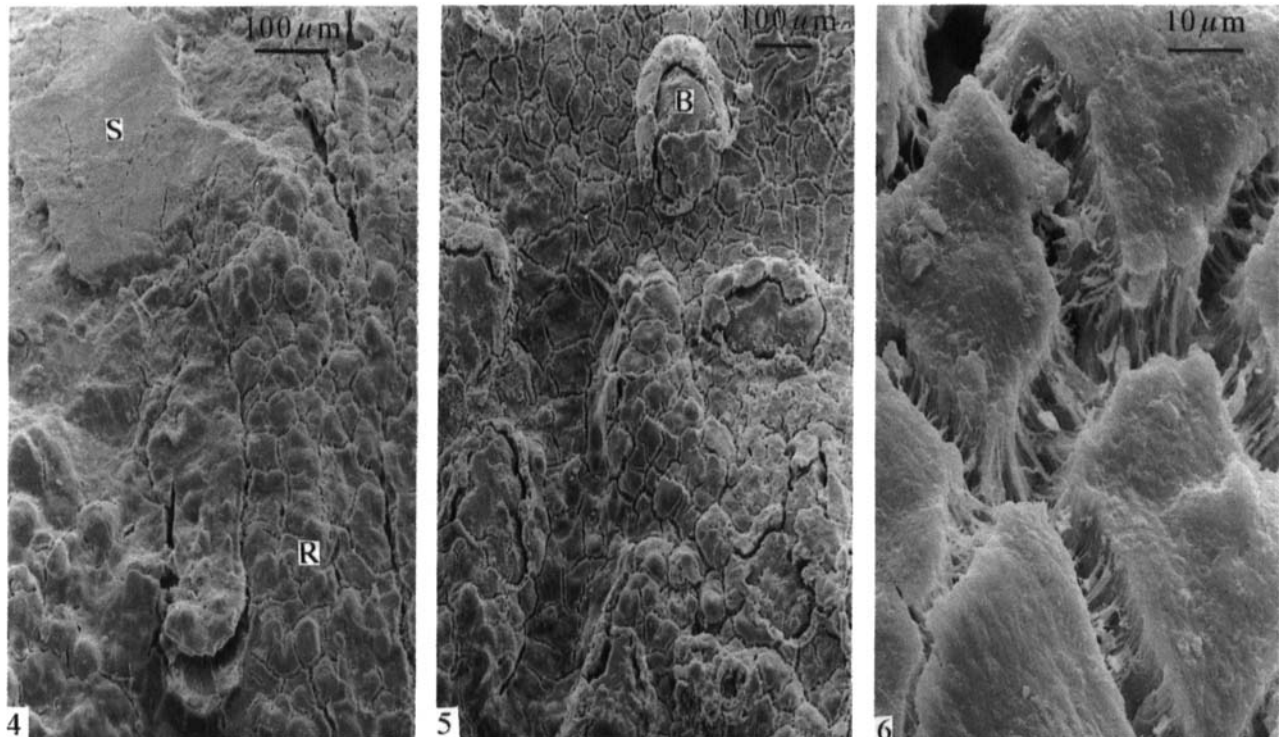
FIGURE 4 Scanning electron micrograph of the surface of the tooth showing apparently worn enamel (S) in the erupted area and some rough enamel (R) in the unerupted area at the bottom of the field of view. Cracks can be seen in both areas.

FIGURE 5 Higher magnification scanning electron micrograph showing blister-like protrusions (B) in the unerupted enamel surface. Extensive cracks partially occluded with a threadlike material bridging their sides can also be seen.

FIGURE 6 Higher magnification scanning electron micrograph of rough unerupted enamel showing extensive cracking and a thread-like material bridging the cracks.



**FIGURE 3** (a) Higher magnification view of an area near the cervical region of the tooth showing the irregular enamel surface. (b) Light micrograph of (a), showing the enamel to be mainly positively birefringent between crossed polarizers except for some negatively birefringent areas (arrowed) near the dentine-enamel-junction.





**FIGURE 7** Transmission electron micrograph showing a variation in crystallite size of the loosely and randomly packed ribbon-like enamel crystals.

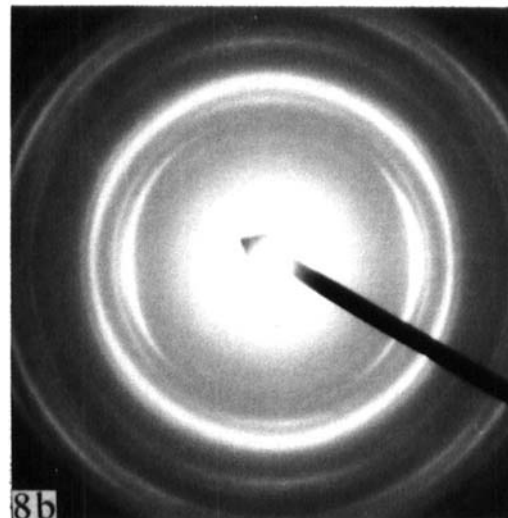
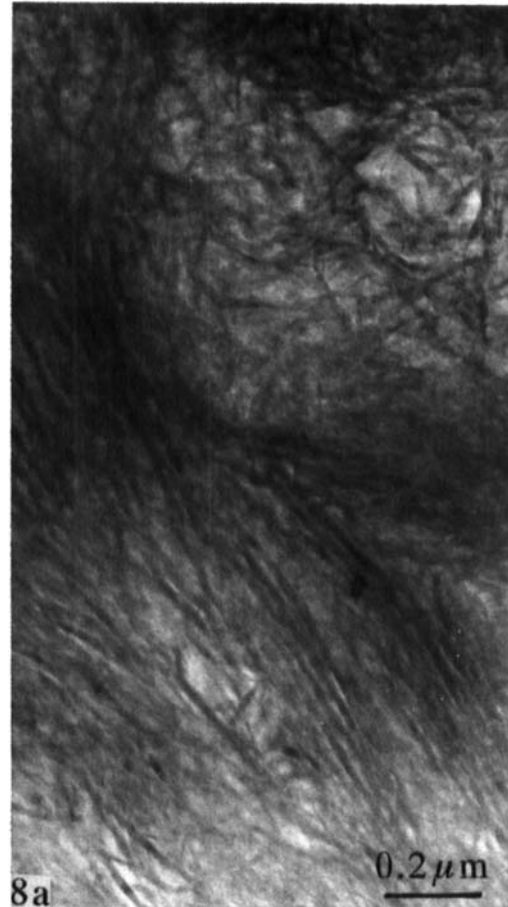


**FIGURE 8** (a) Transmission electron micrograph showing fine ribbon-like enamel crystals in a pseudo-prismatic arrangement. (b) SAD pattern of (a) showing diffuse and discontinuous diffraction rings indicating that the small crystals have some preferred orientation.

the close packing and the random orientation of the ribbon-like crystals in the affected enamel were also different from the close packing of crystals and the well developed prismatic structure of the normal healthy enamel. The affected enamel was also considerably porous compared to the normal healthy enamel. The ultrastructure of the affected enamel suggested that once the initially nucleated crystals became ribbon-like their growth was hindered and the crystals failed to achieve the size and packing of the mature enamel crystals resulting in a hypomaturation type of defect. The presence of some pockets in the affected enamel in which the closely packed crystals were smaller (width ~5 nm) than the ribbon-like crystals suggested that some degree of hypocalcification could also be manifest.

Our electron microscope observations and SAD analysis could not determine whether the affected enamel contained amorphous and/or organic material. However the hypoplastic and hypomatured nature of affected

enamel suggested that it could contain a relatively high unresorbed organic matrix. It could, therefore, be suggested that the cracks observed on the affected enamel could be due to the shrinkage and that the thread-like material in the cracks were artefacts of the cracking process of the organic rich enamel. However, this suggestion seems unlikely because such features have not been observed in dentine or cementum both of which have a similar crystallite size and a high organic component.

The ultrastructure of the affected enamel, revealed by our investigations, strongly points to a genetic disorder or other factors causing hypocalcification and hypomaturation of the enamel crystals, in addition to hypoplasia of the enamel matrix. The presence of hypoplasia hypocalcification and/or hypomaturation defects indicated that both secretory and maturation defects were present in the same tooth. We were unable to find any abnormalities in osteocalcin levels as reported by Lubinsky *et al.*<sup>9</sup> Nephrocalcinosis has been reported to occur as a result of interstitial nephrocalcinosis.<sup>25</sup> The presence of unexplained cellular infiltration in the kidneys of our two patients despite the absence of any history of urinary infection in the boy together with a defect in amelogenesis, suggests the possibility of an underlying abnormality in interstitial matrix leading to dystrophic calcification in the kidneys and abnormal enamel production in the teeth. Alternatively two separate, but closely linked genes could be involved.

#### ACKNOWLEDGMENTS

The authors wish to acknowledge the help given by the Educational Resource Centre and the Department of Radiology, Royal Children's Hospital Melbourne and Drs. H. J. Orams and A. Dickinson.

#### REFERENCES

1. Witkop, C. J. Jr. (1989). *J. Oral Pathol.* **17**, 547.
2. Witkop, C. J. Jr., Sauk, J. J. Jr. (1976). In: *Oral Facial Genetics*, edited by R. E. Stewart and G. H. Prescott, Mosby, St. Louis, pp 151-226.
3. Sundelland, S., and Koch, G. (1985). *Swed. Dent. J.* **9**, 157.
4. Bäckman, B., and Holm, A-K. (1956). *Community. Dent. Oral. Epidemiol.* **14**, 43.
5. Witkop, C. J. (1957). *Acta Genet.* **7**, 236.
6. Wright, J. T., Robinson, C., Shore, R. (1991). *Oral. Surg. Oral. Med. Oral. Pathol.* **72**, 594.
7. Wright, J. T., and Butler, W. T. (1989). *J. Dent. Res.* **68**, 1328.
8. Wright, J. T., Lord, V., Robinson, C., Shore, R. (1992). *J. Oral. Pathol. Med.* **21**, 390.
9. Lubinsky, M., Angle, C., Waynemarsh, P., Witkop, C. J. Jr., (1985). *Am. J. Med. Genet.* **20**, 233.
10. MacGibbon, D. (1972). *Aust. Dent. J.* **17**, 61.
11. Kerebel, B., and Daculsi, G. (1976). *J. Biol. Buccale.* **4**, 43.
12. Kerebel, B., and Daculsi, G. (1977). *Calc. Tiss. Res.* **24**, 191.
13. Phakey, P. P., Rachinger, W. A., Orams, H. J., Carmichael, G. C. (1974). In: *Electron Microscopy*, Vol 1, edited by J. V. Sander and D. J. Goodchild, Australian Academy of Science, Canberra, pp 412-413.
14. Orams, H. J., Phakey, P. P., Rachinger, W. A., Zybert, J. (1974). *Nature* **252**, 584.
15. Orams, H. J., Zybert, J. J., Phakey, P. P., Rachinger, W. A. (1976). *Arch. Oral. Biol.* **21**, 663.
16. Palamara, J., Phakey, P. P., Rachinger, W. A., Orams, H. J. (1980). *Arch. Oral. Biol.* **25**, 715.
17. Palamara, J., Phakey, P. P., Rachinger, W. A., Orams, H. J. (1989). *Adv. Dent. Res.* **3**, 249.
18. Orams, H. J., Phakey, P. P., Rachinger, W. A., Zybert, J. J. (1980). *J. Oral. Pathol.* **9**, 54.
19. Palamara, J., Phakey, P. P., Rachinger, W. A., Orams, H. J. (1986). *J. Oral. Pathol.* **15**, 28.
20. Palamara, J., Phakey, P. P., Rachinger, W. A., Orams, H. J. (1986). *J. Oral. Pathol.* **15**, 109.
21. Rodda, J. C., Palamara, J., Phakey, P. P., Smillie, A. C. (1989). *Arch. Oral. Biol.* **34**, 475.
22. Wright, J. T., Robinson, C., Kirkham, J. (1992). *Pediatr. Dent.* **14**, 331.
23. Sauk, J. J. Jr., Cotton, W. R., Lyon, H. W., Witkop, C. J. Jr. (1972). *Arch. Oral. Biol.* **17**, 771.
24. Hall, R. K., Phakey, P., Palamara, J., McCredie, D. A. (1994). *Oral. Surg. Oral. Med. Oral. Pathol.*, in press.
25. Kessel, D., Hall, C. M., Shaw, D. G. (1992). *Pediatr. Radiol.* **22**, 470.